On the Critical Marangoni Numbers and Dopant Distribution in Silicon Fiber Grown From the Melt by the EFG Technique

LILIANA BRAESCU [a] and THOMAS F. GEORGE [b]
[a] Department of Computer Science
West University of Timisoara
Blv. V. Parvan 4, Timisoara, 300223
ROMANIA

[b] Office of the Chancellor and Center for Nanoscience
Departments of Chemistry & Biochemistry and Physics & Astronomy
University of Missouri–St. Louis
St. Louis, MO 63121
USA

Abstract: - The dependence of the Marangoni flow and impurity distribution on the vertical temperature gradient is analyzed in the framework of a stationary model including the incompressible Navier-Stokes equation in the Boussinesq approximation and the convection-conduction and conservative convection-diffusion equations. The computations are carried out in a 2D axisymmetric model by the finite-element numerical technique, for aluminum-doped silicon fibers grown from the melt by the edge-defined film-fed growth (EFG) technique with central capillary channel shaper and melt replenishment. The Marangoni effect is implemented for the free surface (meniscus) by the weak form-boundary application mode through COMSOL Multiphysics 3.4 software. It is proved numerically that controlling one of the most important process parameters – vertical temperature gradient from the EFG furnace – the best homogeneity of the crystal can be obtained over a wide range of values of the surface tension temperature coefficient.

Key-Words: Finite element technique; fluid flow; Boussinesq approximation; critical Marangoni number; control

1 Introduction

The demand for single or poly-silicon has increased dramatically due to the rapid expansion of the photovoltaic (PV) industry. Various growth techniques have been used for producing silicon wafers for a PV cell, like the Czochralski (Cz), floating zone (Fz) and edge-defined film-fed growth (EFG) methods. Among these, EFG is the first non-conventional technique for crystalline silicon wafer production to enter into large-scale manufacturing in the photovoltaic industry [1], with ribbon growth of silicon meeting the actual demands of economical material consumption because it avoids silicon losses, such as during the blocking of ingots or sawing of wafers [2].

Identifying and investigating the metal impurities in silicon are fundamental tasks in semiconductor physics and device engineering. In solar cells, aluminum is usually present in the metal back contact as well as in the back surface field region. Due to a low diffusivity of interstitial aluminum in silicon, compared to the diffusivity of the transition metals, silicon is intentionally contaminated with aluminum during the growth process. If aluminum is already present as a grown-in impurity in the starting material, then it can act as an electrically-active defect with detrimental consequences to the charge carrier lifetime [3].

Molten silicon is known to be an extremely-reactive material [4], with strong thermal forcing in surface-tension-driven flows being realized during the growth process. The surface tension value and its temperature dependence are essential for describing surface-tension-driven flow (Marangoni-Bénard flow) on the free liquid surface (meniscus, i.e., the liquid bridge between the die and the crystal) [5]. It is generally accepted that thermal fluctuations are a serious drawback in growing a high-quality crystal. The existence of Marangoni convection for molten silicon has been revealed through crystal growth experiments using the Cz [6] and Fz [7] configurations. For the former, the dependence on the Marangoni-Bénard and Rayleigh-Bénard

instabilities on the coefficient dγ/dT of temperature dependence of the surface tension was confirmed. The contribution of the Marangoni effect to the instabilities and consequently to the impurity distribution in the crystal is governed by the magnitude of dγ/dT. Although a large amount of surface tension data has been reported for molten silicon [5], there is still some uncertainty concerning the absolute values and its temperature dependence, because the surface tension of molten silicon is quite sensitive to surface contamination, particularly oxygen. These reasons and the difficulty of an experimental investigation of the surface-tension-driven Marangoni-Bénard convection for small Prandtl numbers (Pr = 0.01 for silicon) have been the motivation for a numerical analysis of the dependence of the Marangoni flow and impurity distribution on the vertical temperature gradient. The computations are carried out in the stationary case in a 2D axisymmetric model by the finite-element numerical technique using COMSOL Multiphysics 3.4 software, for 38 different values of dγ/dT situated in the maximal range [-7×10^{-4}; 0] $Nm^{-1}K^{-1}$ (i.e., for Marangoni numbers Ma between zero and 406.25), which contains all values reported in literature [5], and for three representative vertical temperature gradients in the furnace: k_{g1} = 5,000; k_{g2} = 50,000; k_{g3} = 100,000 Km^{-1} situated in the range [5,000; 100,000] Km^{-1} determined by experimental data [8]. The numerical investigations prove the existence of three critical Marangoni numbers – Ma_{c1}, Ma_{c2}, Ma_{c3} – as reported for two-dimensional containers [9-11]. The best homogeneity of the dopant distribution in the crystal is obtained for Marangoni numbers situated in the first range [0; Ma_{c1}], where the downward flow (dγ/dT < 0) on the free liquid surface leads to a steady fluid flow. The length of this range increases if the vertical temperature gradient in the furnace decreases. This shows that the Marangoni-Bénard instability can be controlled by a delay of the Marangoni convection [12], in order to optimize the crystal quality.

2 The Mathematical Model

The Marangoni flow and impurity distribution induced by vertical temperature gradients in the furnace is analyzed in the framework of a stationary model including the incompressible Navier-Stokes equation in the Boussinesq approximation (the temperature-dependent density appears only in the gravitational force term), and the convection-conduction and conservative convection-diffusion equations [13]:

$$\begin{cases} \rho_l(\bar{\boldsymbol{u}}\cdot\nabla)\bar{\boldsymbol{u}} = \nabla\cdot\left[-p\boldsymbol{I}+\eta\left(\nabla\bar{\boldsymbol{u}}+\left(\nabla\bar{\boldsymbol{u}}\right)^T\right)\right]+\beta\rho_l\,\bar{\boldsymbol{g}}\cdot(T-\Delta T) \\ \nabla\cdot\bar{\boldsymbol{u}} = 0 \\ \nabla\cdot(-k\nabla T+\rho_l C_p T\bar{\boldsymbol{u}}) = 0 \\ \nabla\cdot(-D\nabla c+c\bar{\boldsymbol{u}}) = 0 \end{cases} . \tag{1}$$

The axis-symmetric solutions are searched in the cylindrical-polar coordinate system (rOz) (see Fig. 1). In this system, the unknowns are: velocity vector

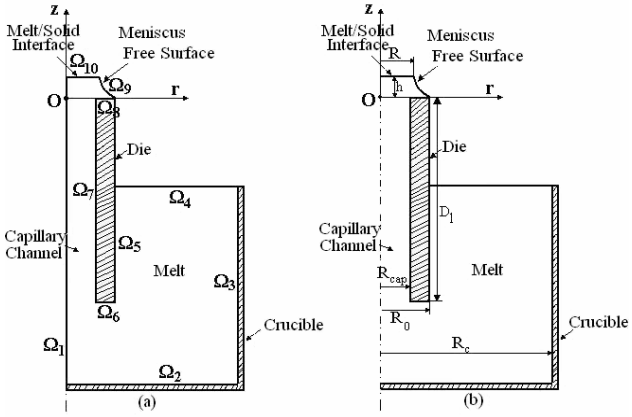

Fig. 1: Schematic EFG crystal growth system showing the domain boundaries (a) and dimensions (b) used in the numerical model.

$\bar{\boldsymbol{u}}$ = (u,v), temperature T, impurity concentration c, and pressure p. The material parameters are: ρ_l - reference melt density, β - heat expansion coefficient, η - dynamical viscosity, k - thermal conductivity, C_p - heat capacity, D - impurity diffusion, and $\bar{\boldsymbol{g}}$ - gravitational acceleration. The system (1) is considered in the two-dimensional domain whose boundary is from Ω_1 to Ω_{10}, as represented on Fig. 1(a).

The fluid density is assumed to vary with temperature as

$$\rho(r,z) = \rho_l\left[1-\beta\left(T(r,z)-\Delta T\right)\right], \tag{2}$$

and the surface tension γ in the meniscus is assumed to vary linearly with temperature as

$$\gamma(r,z) = \gamma_l + \frac{d\gamma}{dT}\left(T(r,z)-\Delta T\right) , \tag{3}$$

where $\Delta T = (T_0+T_m)/2$ is the reference temperature at the free surface, γ_l is the surface tension at the temperature ΔT, and dγ/dT is the rate of change of surface tension with the temperature. The main parameter of the Marangoni-Bénard convection is the Marangoni number

$$Ma = \left|\frac{d\gamma}{dT}\right|\cdot\frac{(T_m-T_0)\cdot h}{\eta\cdot\alpha} , \tag{4}$$

where η is the dynamic viscosity, $\alpha = k/\rho_l C_p$ is the thermal diffusivity, and h the meniscus height.

For solving the system (1), boundary conditions on Ω_1 to Ω_{10} are imposed, with the Oz-axis

considered as a line of symmetry for all field variables:

- *Flow conditions*: On the melt/solid interface, the condition of outflow velocity is imposed, i.e., $\bar{\boldsymbol{u}} = \frac{\rho_l}{\rho_s} v_0 \bar{\boldsymbol{k}}$, where $\bar{\boldsymbol{k}}$ represents the unit vector of the *Oz*-axis. On the melt level in the crucible, the inflow velocity condition is imposed (melt replenishment), $\bar{\boldsymbol{u}} = -\frac{R^2}{R_c^2 - R_0^2} \cdot v_0 \bar{\boldsymbol{k}}$. On the meniscus free surface, we set up the slip/symmetry condition, $\bar{\boldsymbol{u}} \cdot \bar{\boldsymbol{n}} = 0$, $\bar{\boldsymbol{t}} \cdot \left[-p\boldsymbol{I} + \eta\left(\nabla \bar{\boldsymbol{u}} + (\nabla \bar{\boldsymbol{u}})^T\right)\right]\bar{\boldsymbol{n}} = 0$, where $\bar{\boldsymbol{t}}$ and $\bar{\boldsymbol{n}}$ represent the tangential and normal vectors, respectively. The other boundaries are set up by the non-slip condition $\bar{\mathrm{u}} = 0$.
- *Thermal conditions*: On the melt/solid interface, we set the temperature as $T = T_m$. On the free surface, we impose thermal insulation, i.e., $\bar{\boldsymbol{n}} \cdot (-k\nabla T + \rho_l C_p T \bar{\boldsymbol{u}}) = 0$. For the other boundaries, we have the temperature condition $T = T_0$.
- *Concentration conditions*: On the melt/solid interface, the flux condition is imposed, which expresses that impurities are rejected into the melt according to $\frac{\partial c}{\partial \bar{\boldsymbol{n}}} = -\frac{v_0}{D}(1 - K_0)c$. On the melt level in the crucible, the concentration of aluminum in silicon is $c = C_0$. The other boundaries are established by insulation/symmetry, $\bar{\boldsymbol{n}} \cdot (-D\nabla c + c\bar{\boldsymbol{u}}) = 0$.

Imposing the above boundary conditions, on the free surface the Marangoni effect is modeled by using the weak form of the boundary application mode. Thus, on the free surface (meniscus), the boundary condition expresses that the gradient velocity field along the meniscus is balanced by the shear stress,

$$\eta \cdot \begin{bmatrix} t_r & t_z \end{bmatrix} \cdot \begin{bmatrix} 2\frac{\partial u}{\partial r} & \frac{\partial u}{\partial z} + \frac{\partial v}{\partial r} \\ \frac{\partial u}{\partial z} + \frac{\partial v}{\partial r} & 2\frac{\partial v}{\partial r} \end{bmatrix} \cdot \begin{bmatrix} n_r \\ n_z \end{bmatrix} = \frac{d\gamma}{dT} \cdot \left(\frac{\partial T}{\partial r} + \frac{\partial T}{\partial z} \right), \quad (5)$$

where $\bar{\boldsymbol{t}} = (t_r, t_z)$ and $\bar{\boldsymbol{n}} = (n_r, n_z)$. The sign of the rate $d\gamma/dT$, in general, depends on the material, with downward ($d\gamma/dT < 0$) or upward ($d\gamma/dT > 0$) flow on the free liquid surface.

In order to investigate numerically the impurity distribution induced by the Marangoni convection and vertical temperature gradients k_g, we consider 38 values of $\mathrm{d}\gamma/\mathrm{d}T$ situated in the range $[-7\times10^{-4};\ 0]$ $\mathrm{Nm^{-1}K^{-1}}$, and three representative values of k_{g1} = 5,000, k_{g2} = 50,000 and k_{g3} = 100,000 $\mathrm{Km^{-1}}$ situated in the range [5,000; 100,000] $\mathrm{Km^{-1}}$. For every value of the vertical temperature gradient, the dependence of the fluid flow and dopant distribution on the corresponding 38 Marangoni numbers is established. The critical Marangoni numbers are found, following the computed steady or turbulent behavior of the fluid flow. In these numerical investigations, the considered diffusion coefficient of aluminum in liquid silicon is that reported recently by the new determinations of Garandet [4]. The material parameters used in the mathematical model for the considered EFG system are given in Table 1 (Refs. [4,5,8,14]).

Table 1: Material parameters for silicon.

Description (units)		Value
β	heat expansion coefficient ($\mathrm{K^{-1}}$)	5.5×10^{-6}
c	impurity concentration (%)	
C_0	alloy concentration (%)	
C_p	heat capacity ($\mathrm{J\ kg^{-1}K^{-1}}$)	1040
$\mathrm{d}\gamma/\mathrm{d}T$	rate change of the surface tension ($\mathrm{N\ m^{-1}K^{-1}}$)	See text
D	impurity diffusion ($\mathrm{m^2s^{-1}}$)	5.8×10^{-8}
D_l	die length (m)	45×10^{-3}
g	gravitational acceleration ($\mathrm{m\ s^{-2}}$)	9.81
h	meniscus height (m)	0.5×10^{-3}
k	thermal conductivity ($\mathrm{W\ m^{-1}K^{-1}}$)	64
k_g	vertical temp. gradient ($\mathrm{K\ m^{-1}}$)	50000
K_0	partition coefficient	0.002
η	dynamical viscosity ($\mathrm{kg\ m^{-1}s^{-1}}$)	7×10^{-4}
R	crystal radius (m)	1.5×10^{-3}
R_cap	capillary channel radius (m)	0.5×10^{-3}
R_c	inner radius of the crucible (m)	23×10^{-3}
R_0	die radius (m)	2×10^{-3}
ρ_l	density of the melt ($\mathrm{kg\ m^{-3}}$)	2550
$\bar{\boldsymbol{u}}$	velocity vector	
v_0	pulling rate ($\mathrm{m\ s^{-1}}$)	1×10^{-7}
T	temperature (K)	
T_0	temperature at $z = h$ (K)	
T_m	melting temperature (K)	1685
ΔT	reference temperature (K)	
z	coord. in the pulling direction	

3 Numerical results

The computations are made using the two-dimensional axis-symmetric hypothesis for an aluminum-doped silicon ribbon of radius R = 1.5×10^{-3} m grown with a pulling rate $v_0 = 10^{-7}$ $\mathrm{ms^{-1}}$. The boundaries presented in Fig. 1 are determined from the peculiarities of the considered EFG growth system. Thus, a crucible with inner radius R_c = 23×10^{-3} m is considered, which is continuously fed with the melt, such that the melt height in the crucible is maintained as constant at 45×10^{-3} m. In

the crucible, a die with radius $R_0 = 2\times10^{-3}$ m and length is introduced, such that 2/3 of the die 45×10^{-3} m is immersed in the melt. In the die, a capillary channel of radius $R_{cap} = 0.5\times10^{-3}$ m, i.e., capillary number $Ca = 5.5\times10^{-5}$, is manufactured through which the melt rises to the top of the die, where a small meniscus of height $h = 0.5\times10^{-3}$ m is formed.

The stationary incompressible Navier-Stokes model for fluid flow, stationary heat transfer and mass transfer, along with the weak form of the boundary condition are implemented with the COMSOL Multiphysics 3.4 software, and the system (1) is solved by the finite-element numerical technique. According to the considered geometry, 17,072 triangular elements and 150,803 degrees of freedom are considered. The effect of the Marangoni forces is computed in the stationary case for the three values $k_{g1} = 5{,}000$, $k_{g2} = 50{,}000$ and $k_{g3} = 100{,}000$ Km^{-1} of the vertical temperature gradient in the furnace situated in the range [5,000; 100,000] Km^{-1} and for different Marangoni numbers Ma situated in the range [0; 406.25] (see Eq. (4)), which corresponds to those 38 considered values of the surface tension rates.

The computed fluid flows and their behaviors (downward steady flow, appearance of small turbulences, and increasing of turbulences in the meniscus) reveal the following critical Marangoni numbers Ma_c which depend on the vertical temperature gradients:

1. For $k_{g1} = 5{,}000$ Km^{-1}, there is only one Ma_c value ($Ma_{c1} = 75.4$) situated in the range [0; 406.25];
2. For $k_{g2} = 50{,}000$ Km^{-1}, there are three values of Ma_c situated in the range [0; 406.25]: $Ma_{c1} = 7.54$, $Ma_{c2} = 39.46$ and $Ma_{c3} = 69.64$;
3. For $k_{g3} = 100{,}000$ Km^{-1}, the values of Ma_c are: $Ma_{c1} = 3.65$, $Ma_{c2} = 19.73$ and $Ma_{c3} = 35.4$.

These critical values are essential in the fluid flow behavior and in the dopant concentration.

For the considered vertical temperature gradients k_{g1}, k_{g2} and k_{g3}, if Ma is situated in the first range [0; Ma_{c1}], then the steady downward flow ($d\gamma/dT < 0$) on the free liquid surface push the maximum of the dopant concentration C_{max} at the triple-point, as it can be seen in Figs. 2 & 3(a-c). The computed fluid velocity distribution shows that in the case for which we consider the forced flow, i.e., $Ma = 0$ (see Fig. 2), with a rate of 10^{-7} ms^{-1} at the solid-liquid interface (the pulling rate) if the ratio ρ_l/ρ_s is neglected, and consequently 9×10^{-7} ms^{-1} on average in the capillary channel (taking into account the surface ratio between crystal and channel), then the maximum forced velocity is 18×10^{-7} ms^{-1}. This maximum is situated in the center of the capillary channel; if the vertical temperature gradient increases, then perturbations appear.

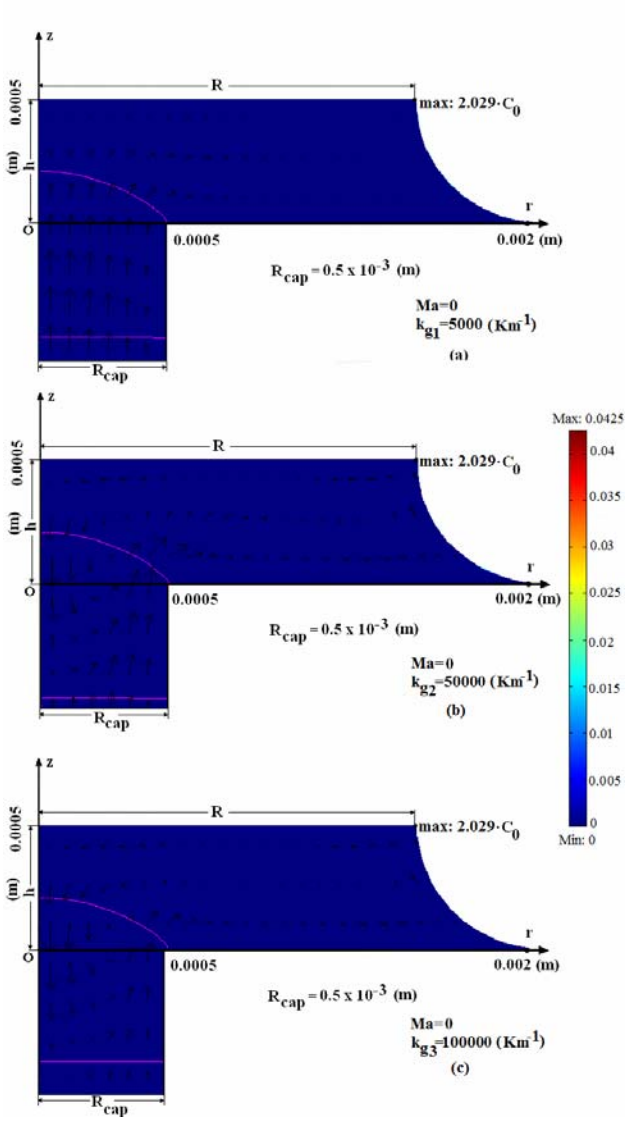

Figure 2: Computed fluid flows and maximum values of the dopant distribution for the Marangoni number $Ma = 0$ in the case of $k_{g1} = 5{,}000$ Km^{-1} (a), $k_{g2} = 50{,}000$ Km^{-1} (b) and $k_{g3} = 100{,}000$ Km^{-1} (c).

For the case in which the surface driven flows are taken into account (Fig. 3), the Marangoni convection perturbs the forced flow: the arrows presented in Fig. 3 denote the flow of the velocity field caused by the surface tension driven flow (downward flow on the meniscus). The maximum velocity of the fluid flow in the meniscus is situated on the free surface, and it increases if the Marangoni number increases. This dependence and the magnitude of the maximum velocity are in agreement with the equilibrium of the viscous and Marangoni forces,

$$U \approx Ma \cdot \frac{\upsilon}{h} ,$$

where v is the kinematic viscosity [13].

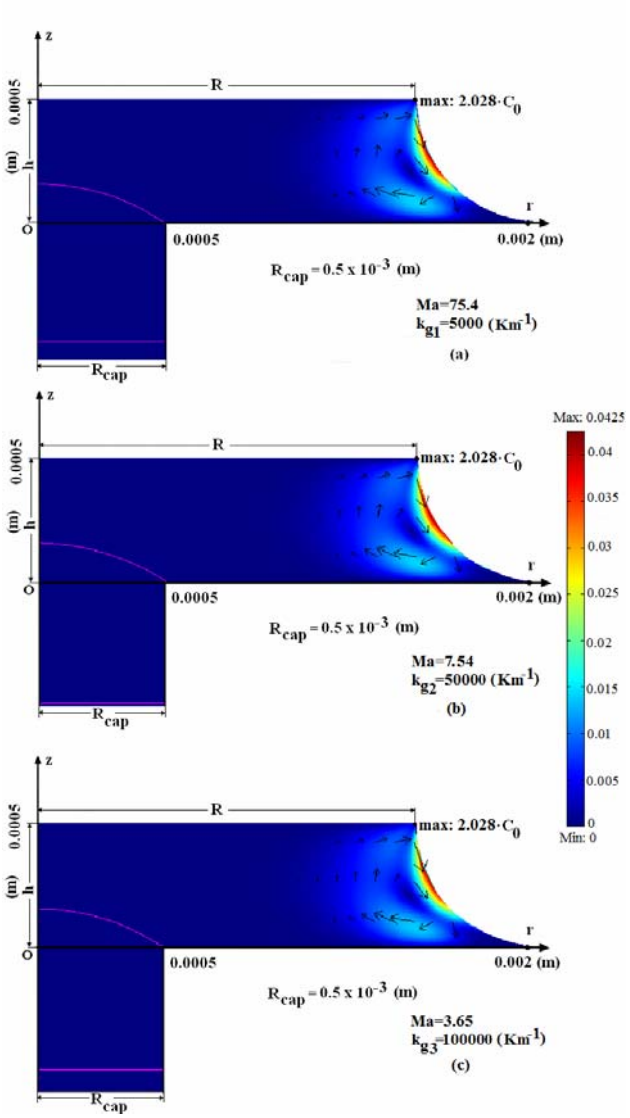

Figure 3: Computed fluid flows and maximum values of the dopant distribution for the first critical Marangoni numbers Ma_{c1} in the case of k_{g1} = 5,000 Km^{-1} (a), k_{g2} = 50,000 Km^{-1} (b) and k_{g3} = 100,000 Km^{-1} (c).

These behaviors of the fluid flow show that if Ma increases in the corresponding ranges [0; Ma_{c1}], then a better mixing of the dopant distribution takes place near the free meniscus surface, and hence C_{max} decreases slowly from 2.029×C_0 (which corresponds to Ma = 0, Fig. 2) to 2.028×C_0 (which corresponds to Ma= Ma_{c1}, Fig. 3).

These investigations prove that, for any vertical temperature gradients k_{g1}, k_{g2} and k_{g3}, the fluids flow and dopant distributions are similar for Ma in the range [0; Ma_{c1}]. The most important point is the length of the interval [0; Ma_{c1}], which depends on the size of the vertical temperature gradient. For practical crystal growers, this information offers the possibility to change the configuration of the equipment and process parameters (vertical temperature gradient) for optimization of the crystal quality.

Concerning of the second (Ma_{c2}) and third (Ma_{c3}) critical Marangoni numbers, computations show that if Ma increases in the ranges (Ma_{c1}; Ma_{c2}], (Ma_{c2}; Ma_{c3}] and (Ma_{c3}; 406.25] for k_{g2} and k_{g3}, or if Ma increases in the range (Ma_{c1}; 406.25] for k_{g1}, the velocity of the fluid flow in the meniscus increases, and turbulences in the fluid flow take place. More precisely, if Ma increases in the range (Ma_{c1}; Ma_{c2}] for k_{g2} and k_{g3} (or if Ma increases in the range (Ma_{c1}; 406.25] for k_{g1}) then very small turbulences in the fluid flow lead to an increase of C_{max}, which is located at the triple-point. If Ma increases in the range (Ma_{c2}; Ma_{c3}], then turbulences in the fluid increase, and C_{max} is pushed inside at the level of the melt/crystal interface, at a distance on the same order as the meniscus height from the external crystal surface (see Fig. 4).

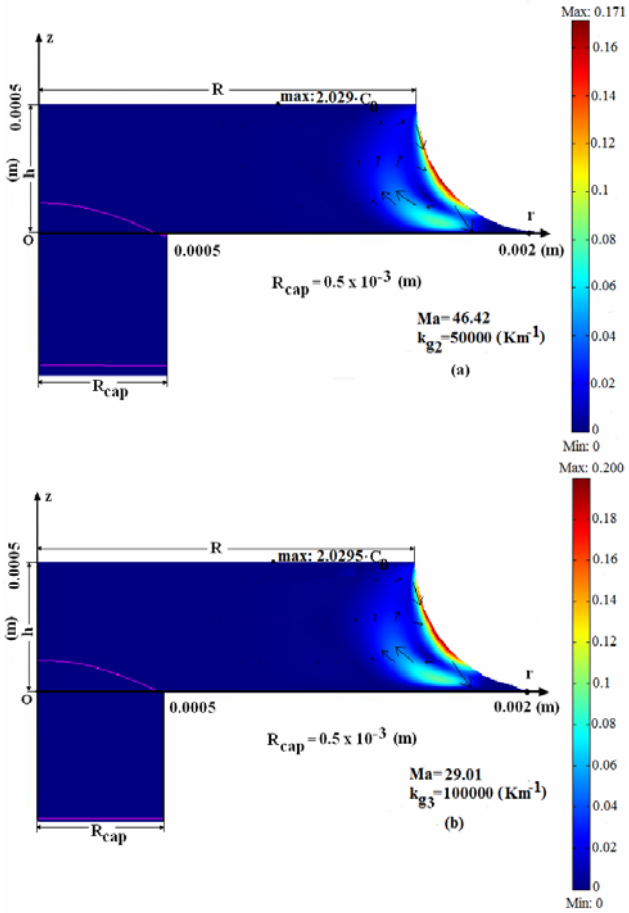

Figure 4: Computed fluid flows and maximum values of the dopant distribution for the Marangoni numbers in the range (Ma_{c2}; Ma_{c3}]: Ma = 46.42 for k_{g2} = 50,000 Km^{-1} (a) and Ma = 29.01 for k_{g3} = 100,000 Km^{-1} (b).

If Ma increases in the range (Ma_{c3}; 406.25],

then higher turbulences move C_{max} at the triple-point which increases considerably.

Investigations show that for smaller vertical temperature gradients we obtain a wide range [0; Ma_{c1}] of values of the surface tension temperature coefficients which assures the best homogeneity of the crystal.

4 Conclusions

The dependences of the Marangoni flow and impurity distribution on the vertical temperature gradient in aluminum-doped silicon fibers, grown from the melt by the EFG method, are determined numerically by the finite-element technique in the framework of a stationary model including incompressible fluid flow in the Boussinesq approximation, heat and mass transfer, and the Marangoni effect. The computed fluid flows and their behaviors (downward steady flow, appearance of small turbulences, and increasing of turbulences in the meniscus) reveal the existence of three critical Marangoni numbers, Ma_{c1}, Ma_{c2} and Ma_{c3}, which depend on the vertical temperature gradients. The wide range [0; Ma_{c1}] over which the downward steady flow induce the best homogeneity of the dopant distribution is obtained for the smaller considered vertical temperature gradient. This suggests to practical crystal growers that a possible feedback control for delaying the Marangoni convection can be obtained by decreasing vertical temperature gradient in the furnace. This control can be realized by other choices of the process parameters, e.g., by applying magnetic fields [15], which suggest further developments near the future.

Acknowledgment

We are grateful to the North Atlantic Treaty Organisation (Grant CBP.EAP.CLG 982530) for support of this project.

References:

[1] B. Yang, L. L. Zheng, B. Mackintosh, D. Yates, J. Kalejs, Meniscus dynamics and melt solidification in the EFG silicon tube growth process, *Journal of Crystal Growth*, Vol. 293, 2006, pp. 509-516.

[2] H. Kasjanow, A. Nikanorov, B. Nacke, H. Behnken, D. Franke, A. Seidl, 3D coupled electromagnetic and thermal modeling of EFG silicon tube growth, *Journal of Crystal Growth*, Vol. 303, 2007, pp. 175-179.

[3] P. Rosenits, T. Roth, S. Glunz, S. Beljakowa, Determining the defect parameters of the deep aluminum-related defect center silicon, *Applied Physics Letters*, Vol. 91, 2007, pp. 122109:1-3.

[4] J. P. Garandet, New determinations of diffusion coefficients for various dopants in liquid silicon, *International Journal of Thermophysics*, Vol. 28/4, 2007, pp. 1285-1303.

[5] M. Przyborowski, T. Hibiya, M. Eguchi, I. Egry, Surface tension measurement of molten silicon by the oscillating drop method using electromagnetic levitation, *Journal of Crystal Growth*, Vol.151, 1995, pp. 60-65.

[6] K.-W. Yi, K. Kakimoto, M. Eguchi, M. Watanabe, T. Shyo, T. Hibiya, Spoke patterns on molten silicon in Czochralski system, *Journal of Crystal Growth*, Vol. 144/1-2, 1994, pp. 20-28.

[7] S. Nakamura, T. Hibiya, K. Kakimoto, N. Imaishi, S. Nishizawa, A. Hirata, K. Mukai, S. Yoda, T. S. Morita, Temperature fluctuations of the Marangoni flow in a liquid bridge of molten silicon under microgravity on board the TR-IA-4 rocket, *Journal of Crystal Growth*, Vol.186, 1998, pp. 85-94.

[8] O. Bunoiu, I. Nicoara, J. L. Santailler and T. Duffar, Fluid flow and solute segregation in EFG crystal growth process, *Journal of Crystal Growth*, Vol. 275, 2005, pp. e799-e805.

[9] T. Boeck, A. Thess, Inertial Benard-Marangoni convection, *Journal of Fluid Mechanics* Vol. 350, 1997, pp. 149-175.

[10] K. A. Cliffe, S. J. Tavener, Marangoni-Benard convection with a deformable free surface, *Journal of Computational Physics*, Vol. 145, 1998, pp. 193-227.

[11] T. Boeck, Bénard-Marangoni convection at large Marangoni numbers: results of numerical simulations, *Advances in Space Research*, Vol. 36, 2005, pp. 4-10.

[12] N. M. Arifin, R. M. Nazar, N. Senu, Feedback control on the Marangoni-Bénard instability in a fluid layer with a free-slip bottom, *Journal of the Physical Society of Japan*, Vol.76/1, 2007, pp. 014401:1-4.

[13] L. Braescu, T. Duffar, Effect of buoyancy and Marangoni forces on the dopant distribution in a single crystal fiber grown from the melt by edge-defined film-fed growth (EFG) method, *Journal of Crystal Growth*, Vol. 310, 2008, pp. 484-489.

[14] J. P. Kalejs, Modeling contributions in commercialization of silicon ribbon growth from the melt, *Journal of Crystal Growth*, Vol. 230, 2001, pp. 10-21.

[15] P. Dold, A. Croll, K. W. Benz, Floating-zone growth of silicon in magnetic fields. I. Weak static axial fields, *Journal of Crystal Growth*, Vol.183, 1998, pp. 545-553.